

## BCCIP Suppresses Tumor Initiation but Is Required for Tumor Progression

Yi-Yuan Huang, Li Dai, Dakim Gaines, Roberto Droz-Rosario, Huimei Lu, Jingmei Liu, and Zhiyuan Shen

### Abstract

Dysfunctions of genome caretaker genes contribute to genomic instability and tumor initiation. Because many of the caretaker genes are also essential for cell viability, permanent loss of function of these genes would prohibit further tumor progression. How essential caretaker genes contribute to tumorigenesis is not fully understood. Here, we report a "hit-and-run" mode of action for an essential caretaker gene in tumorigenesis. Using a BRCA2-interacting protein BCCIP as the platform, we found that a conditional BCCIP knockdown and concomitant p53 deletion caused rapid development of medulloblastomas, which bear a wide spectrum of alterations involving the Sonic Hedgehog (Shh) pathway, consistent with a caretaker responsibility of BCCIP on genomic integrity. Surprisingly, the progressed tumors have spontaneously lost the transgenic BCCIP knockdown cassette and restored BCCIP expression. Thus, a transient downregulation of BCCIP, but not necessarily a permanent mutation, is sufficient to initiate tumorigenesis. After the malignant transformation has been accomplished and autonomous cancer growth has been established, BCCIP reverses its role from a tumor-initiation suppressor to become a requisite for progression. This exemplifies a new type of tumor suppressor, which is distinct from the classical tumor suppressors that are often permanently abrogated during tumorigenesis. It has major implications on how a nonmutagenic or transient regulation of essential caretaker gene contributes to tumorigenesis. We further suggest that BCCIP represents a paradoxical class of modulators for tumorigenesis as a suppressor for initiation but a requisite for progression (SIRP). *Cancer Res*; 73(23); 7122–33. ©2013 AACR.

### Introduction

Genomic instability is one of the enabling characters during tumorigenesis (1). It can be caused by dysregulations in DNA repair, compromised DNA replication fidelity, imprecise chromosome segregation during mitosis, improper cell-cycle coordination, and so on (2). A tumor-suppressor gene involved in the maintenance of genomic integrity is often referred to as a caretaker (3). Although defective caretakers may not immediately promote tumor growth, they cause stochastic genomic alterations that increase the risk of inactivating gatekeeper tumor suppressors and activations of growth-promoting oncogenes. The loss of gatekeeper functions and activation of

progrowth oncogenes then causes oncogenic transformation and imminent tumor growth and progression. Theoretically, when the defects of caretakers have caused the activation of autonomous progrowth pathways and malignant transformation, the caretaker deficiency may no longer be a requisite for subsequent tumor progression. Thus, caretaker defects may act in a "hit-and-run" manner to initiate tumorigenesis, and it is possible that only a transient dysfunction may be sufficient to trigger tumorigenesis. However, experimental evidence of such prediction is rare.

Many of the DNA repair genes are not only critical for the maintenance of genomic integrity but are also essential for cell viability and proliferation because of their fundamental involvement in DNA replication and mitosis. Therefore, a permanent inactivation of these genes may prohibit tumor progression despite its contribution to the initiation of tumorigenesis. There has been a conundrum on how these viability-essential caretaker genes modulate tumorigenesis. In this study, we constructed a conditional *BCCIP* knockdown transgenic mouse model. In this model, the expression of *BCCIP* is downregulated by shRNA but can be restored when a spontaneous deletion of the knockdown cassette occurs due to growth pressure during tumor progression. We found that *BCCIP* modulates tumorigenesis in an unconventional way: it serves as a tumor suppressor, but later is required for tumor progression.

*BCCIP* was originally identified as a BRCA2 and CDKN1A (Cip1/waf1/p21) interacting protein (4). Knockdown of *BCCIP* caused significant reduction of homologous recombination (5, 6), spontaneous chromatid aberrations including single

**Authors' Affiliation:** Rutgers Cancer Institute of New Jersey, Department of Radiation Oncology, Rutgers Robert Wood Johnson Medical School, Rutgers, The State University of New Jersey, New Brunswick, New Jersey

**Note:** Supplementary data for this article are available at Cancer Research Online (<http://cancerres.aacrjournals.org/>).

Current address for Y.-Y. Huang: National Institute for Child Health and Human Development (NICHD), National Institutes of Health, Bethesda, Maryland; and current address for L. Dai: College Life Sciences, Zhejiang University, Hangzhou, Zhejiang, China.

**Corresponding Author:** Zhiyuan Shen, Rutgers Cancer Institute of New Jersey, Department of Radiation Oncology, Rutgers Robert Wood Johnson Medical School, The State University of New Jersey, New Brunswick, NJ 08903. Phone: 732-235-6101; Fax: 732-235-7493; E-mail: shenzh@cinj.rutgers.edu

doi: 10.1158/0008-5472.CAN-13-1766

©2013 American Association for Cancer Research.

chromatid breaks and sister chromatid union (7), cytokinesis failure (8), and cell-cycle dysregulation (9–15). In addition, *BCCIP* is an essential gene, and persistent deficiency of *BCCIP* leads to proliferation defects and mitosis failure (7, 8, 14). Downregulation of *BCCIP* expression has been observed in some human cancers (16–18), but significant *BCCIP* mutations have not been reported in cancer tissues. In previous studies, we found that *BCCIP* deficiency caused proliferation arrest among neural progenitor cells, leading to severe neurogenesis defects (14). In this study, we showed that these neurogenesis defects can be rescued by a concomitant deletion of p53 gene. However, this leads to rapid formation of medulloblastoma with activation of the Sonic Hedgehog (Shh) signaling pathway, confirming a caretaker tumor-suppressor responsibility for *BCCIP*. Interestingly, reappearance of *BCCIP* protein expression was found in final-stage medulloblastomas as a result of spontaneous deletion of the *BCCIP* short hairpin RNA (shRNA) expression transgene cassette. Our data suggest that *BCCIP* deficiency works in a "hit-and-run" manner to promote tumorigenesis. Thus, *BCCIP* has a paradoxical role in tumorigenesis—as a suppressor for the initiation and a requisite for the tumor progression when the oncogenic transformation has been accomplished—revealing an unconventional class of modulators for tumorigenesis.

## Materials and Methods

### Mouse strains

The names of mouse lines and their corresponding genotypes used in this study are listed in Table 1. The FVB-*LoxPshBCCIP*<sup>+/-</sup> mice were generated at the transgenic mice

core facility of Rutgers Robert Wood Johnson Medical School as described previously (7). The glial fibrillary acidic protein (GFAP) promoter-driven Cre recombinase (GFAP-Cre) transgenic mice (*FVB-Tg(GFAP-Cre)25Mes/J*) were obtained from the Jackson Laboratory (stock no. 004600). These mice were interbred to obtain BCCIP-CON (*LoxPshBCCIP*<sup>+/-</sup>;*GFAP-Cre*<sup>-/-</sup>) and BCCIP-CKD (*LoxPshBCCIP*<sup>+/-</sup>;*GFAP-Cre*<sup>+/-</sup>) mice. To generate BCCIP-CKD;p53<sup>LoxP/LoxP</sup> (*LoxPshBCCIP*<sup>+/-</sup>; *p53*<sup>LoxP/LoxP</sup>; *GFAP-Cre*<sup>+/-</sup>) mice, the p53-floxed transgenic mice (*B6.129P2-Trp53<sup>tm1Brn</sup>/J*) were obtained from the Jackson Laboratory (stock no. 008462) and then interbred with BCCIP-CKD mice to generate BCCIP-CKD;Trp53<sup>LoxP/wt</sup> (*LoxPshBCCIP*<sup>+/-</sup>; *p53*<sup>LoxP/wt</sup>;*GFAP-Cre*<sup>+/-</sup>) mice, which were then intercrossed with p53-floxed transgenic mice to generate the BCCIP-CKD; p53<sup>LoxP/LoxP</sup> mice. During breeding, the GFAP-Cre transgene was routinely carried by the male to avoid germ-line *BCCIP* disruption due to low level of Cre expression in the ovaries. Mice used in the p53-deficient study resulted from backcrossing mix FVB and B6.129P2. All routine mouse care and handling was approved by and performed according to the guidelines of the institutional animal care committee.

### Western blot analysis

Western blots were performed with procedures as described previously (7). Primary antibodies used were mBCCIP (7), Cre (1:2,000; 69050-3, Novagen), p53 (1:2,000; sc-6243, Santa Cruz Biotechnology), PCNA (1:2,500; sc-53407; Santa Cruz Biotechnology), PTEN (1:1,000, #9559; Cell Signaling Technology), and phospho-PTEN-Ser380 (1:1,000; #9551; Cell Signaling Technology).

**Table 1** Summary of the mouse genotypes, designation used in text, brain size, medulloblastoma incidence, and onset times

Genotypes	Designation in text	Brain size	Incidence of medulloblastoma/ total number of mice	Onset (days) for medulloblastoma
<i>LoxPshBCCIP</i> <sup>-/-</sup> ; <i>p53</i> <sup>wt/wt</sup> ; <i>GFAP-Cre</i> <sup>+/-</sup>	BCCIP-CON;p53 <sup>wt/wt</sup>	Normal	0/32	N/A
<i>LoxPshBCCIP</i> <sup>-/-</sup> ; <i>p53</i> <sup>LoxP/wt</sup> ; <i>GFAP-Cre</i> <sup>+/-</sup>	BCCIP-CON;p53 <sup>LoxP/wt</sup>	Normal	0/31	N/A
<i>LoxPshBCCIP</i> <sup>-/-</sup> ; <i>p53</i> <sup>LoxP/LoxP</sup> ; <i>GFAP-Cre</i> <sup>+/-</sup>	BCCIP-CON;p53 <sup>LoxP/LoxP</sup>	Normal	0/45	N/A
<i>LoxPshBCCIP</i> <sup>+/-</sup> ; <i>p53</i> <sup>wt/wt</sup> ; <i>GFAP-Cre</i> <sup>+/-</sup>	BCCIP-CKD;p53 <sup>wt/wt</sup>	Microcephaly	0/35	N/A
<i>LoxPshBCCIP</i> <sup>+/-</sup> ; <i>p53</i> <sup>LoxP/wt</sup> ; <i>GFAP-Cre</i> <sup>+/-</sup>	BCCIP-CKD;p53 <sup>LoxP/wt</sup>	Reduced Microcephaly	0/29	N/A
<i>LoxPshBCCIP</i> <sup>+/-</sup> ; <i>p53</i> <sup>LoxP/LoxP</sup> ; <i>GFAP-Cre</i> <sup>+/-</sup>	BCCIP-CKD;p53 <sup>LoxP/LoxP</sup>	Normal	45/45	95 ± 15
<i>LoxPshBCCIP</i> <sup>+/-</sup> ; <i>GFAP-Cre</i> <sup>-/-</sup> ; <i>p53</i> <sup>wt/wt</sup>	BCCIP-CON	Normal	(N/A)	N/A
<i>LoxPshBCCIP</i> <sup>+/-</sup> ; <i>GFAP-Cre</i> <sup>+/-</sup> ; <i>p53</i> <sup>wt/wt</sup>	BCCIP-CKD(same as BCCIP-CKD;p53 <sup>wt/wt</sup> )	Microcephaly	(N/A)	N/A
<i>GFAP-Cre</i> <sup>+/-</sup>	GFAP-Cre	Normal	(N/A)	N/A

### Histologic and immunohistochemical analysis

Mice brains were fixed in 10% buffered formalin for 24 to 48 hours before paraffin embedding. All paraffin-embedded sections were cut at a thickness of 5  $\mu$ m. These sections were stained with hematoxylin and eosin (H&E) according to standard procedures. Immunohistochemical analyses of tissue were performed by permeabilizing with 0.1% Triton X-100 in PBS for 10 minutes, quenching endogenous peroxides with 3% hydrogen peroxide for 10 minutes, followed by blocking, as well as primary and secondary antibody incubation. Immunoreactivity was visualized with 3,3'-diaminobenzidine (DAB; D5637; Sigma). Positive staining appears as brown nuclear staining, whereas nuclei counterstained with hematoxylin appear as blue in color. All cryosection immunofluorescence staining was performed after antigen retrieval by boiling in 0.01 mol/L citric acid buffer (pH 6.0). The following primary antibodies were used: calbindin D-28K (1:500; C9848; Sigma), NeuN (1:100; MAB377; Millipore), GFAP (1:400, ab360; Abcam), Ki67 (1:300, ab15580; Abcam), and synaptophysin (1:100, ab8049; Abcam).

### PCR genotyping and quantitative real-time reverse transcriptase PCR analysis

The genotypes (see Table 1 for a list) were identified by PCR of tail snip DNA prepared by using proteinase K digestion and phenol-chloroform extraction. The primers used to screen the genotypes are summarized in Supplementary Table S1. Total RNA was extracted from mouse tissues with the GeneElute Mammalian total RNA miniprep kit (Sigma-RTN70). The complementary DNA was generated with oligo(dT) primers using the Omniscript RT kit (QIAGEN-205111). Real-time PCR was performed in duplicate with TaqMan PCR mixture (Applied Biosystems) in the 7000 ABI sequence detection system. The expression of genes was normalized to the housekeeping gene *GAPDH*. All quantitative PCR (qPCR) primers were part of the preprepared Applied Biosystems TaqMan packages as summarized in Supplementary Table S2.

### cDNA sequencing of BCCIP, PTEN, and Ptch1

The cDNA was synthesized as described previously (7). The paired primers used to amplify the full-length coding regions of *BCCIP* and *PTEN* are listed in Supplementary Table S3. Six overlapping fragments were amplified to cover the full-length coding region of mouse *Ptch1* cDNA using the primer sets listed in Supplementary Table S3, including those previously used by others (19). In addition, these primers were used to sequence the amplified PCR products. For *BCCIP* and *PTEN* cDNA, two additional primers (shown in the last two rows of Supplementary Table S3) were also used for sequencing.

## Results

### Rescue of neurogenesis defects by concurrent p53 deletion in BCCIP conditional knockdown mice

On the chromosome, the *BCCIP* gene overlaps with its neighboring genes (9). To avoid potential interference with genes flanking *BCCIP* by conventional knockout approaches,

we constructed a conditional BCCIP knockdown transgenic mouse line, designated *LoxPshBCCIP* (7). By crossing the *LoxPshBCCIP*<sup>+/+</sup> mice with the GFAP-Cre transgenic mice, we found that BCCIP knockdown caused proliferation defects on embryonic neural progenitors (14). Because BCCIP deficiency caused accumulation of DNA damage in the proliferative progenitor cells and spontaneous p53 activation (7, 14), we asked whether the neurogenesis defects in BCCIP-deficient mice can be rescued by concurrent p53 deletion. We crossed *LoxPshBCCIP* mice with the conditional p53 knockout mice (hereafter designated p53<sup>LoxP/LoxP</sup>; ref. 20), where exons 2 to 10 of the *Trp53* gene are flanked by LoxP sites and can be conditionally deleted by expression of Cre-recombinase. After further crossing with GFAP-Cre mice (21), we generated mice with six genotypes as detailed in the Table 1.

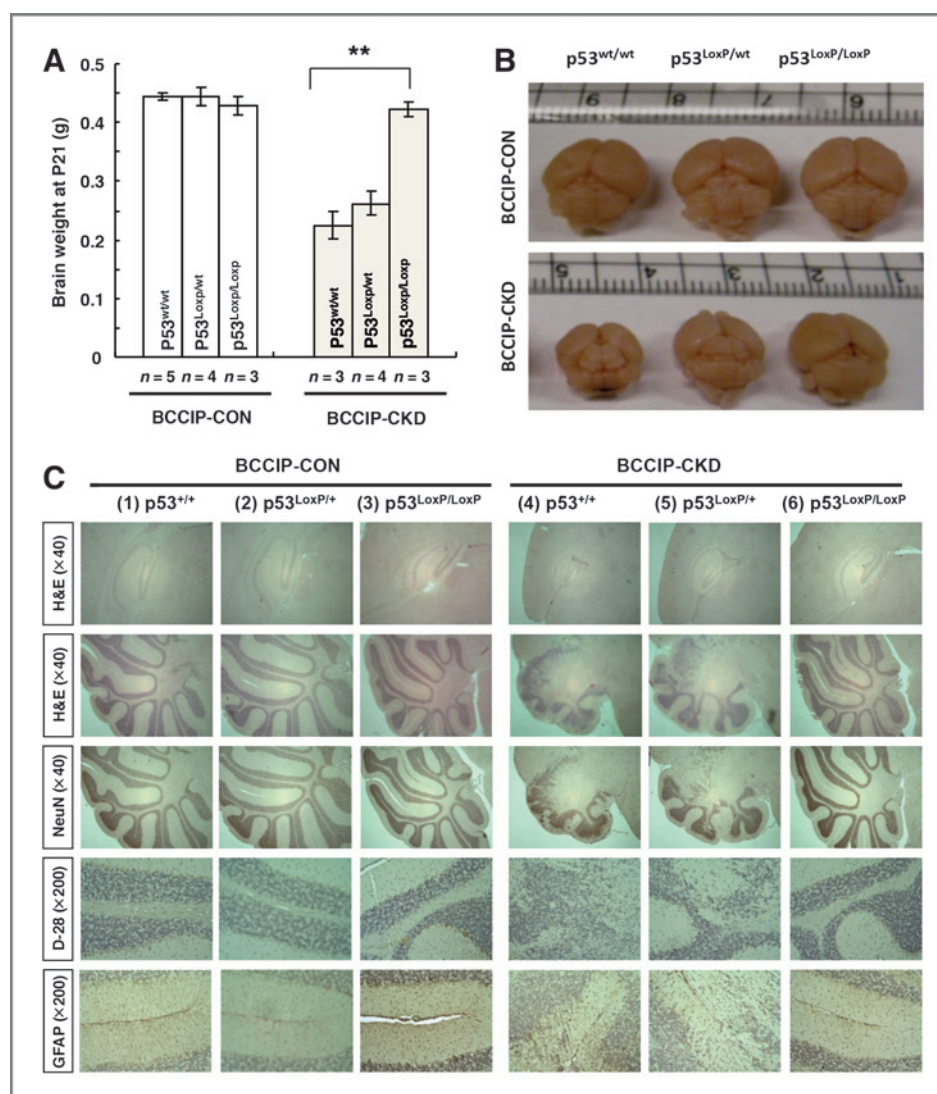
As shown in Fig. 1, the GFAP-Cre-mediated p53 deletion indeed rescued the microcephaly in the BCCIP-CKD mice (Fig. 1A and B), and corrected the abnormal cerebral and cerebellar structures observed in BCCIP-CKD mice (Fig. 1C). In addition, p53 heterozygosity (BCCIP-CKD;p53<sup>LoxP/wt</sup>) partially improved cerebellar development, and slightly corrected the microcephaly (Fig. 1C). Although the BCCIP-CKD mice displayed major motor coordination deficits (14), the BCCIP-CKD;p53<sup>LoxP/LoxP</sup> (*LoxPshBCCIP*<sup>+/-</sup>; p53<sup>LoxP/LoxP</sup>; *GFAP-Cre*<sup>+/-</sup>), mice were able to successfully complete the balance beam test. These observations suggest that p53 is required for the previously reported neurogenesis defects in BCCIP deficient mice, and concurrent p53 deletion rescues the neurodevelopmental deficits.

### Development of medulloblastoma in conditional BCCIP knockdown mice with concurrent p53 deletion

Although the GFAP-Cre-mediated p53 deletion rescued the neurogenesis defects of BCCIP-CKD mice, all of the BCCIP-CKD;p53<sup>LoxP/LoxP</sup> (*LoxPshBCCIP*<sup>+/-</sup>; p53<sup>LoxP/LoxP</sup>; *GFAP-Cre*<sup>+/-</sup>) mice became moribund and were diagnosed with medulloblastoma within the cerebellum with an average onset at 95 days of age (Fig. 2A and B; Table 1). However, medulloblastomas were not present in BCCIP-CKD;p53<sup>wt/wt</sup> (*LoxPshBCCIP*<sup>+/-</sup>; p53<sup>wt/wt</sup>; *GFAP-Cre*<sup>+/-</sup>) or in the BCCIP-CON;p53<sup>LoxP/LoxP</sup> (*LoxPshBCCIP*<sup>-/-</sup>; p53<sup>LoxP/LoxP</sup>; *GFAP-Cre*<sup>+/-</sup>) mice, when observed throughout their lifespan. Necropsy and histology studies illustrated that the medulloblastoma foci are within the external granular layer of the cerebellum (Fig. 2B). The tumor tissues are immune-positive for synaptophysin, a marker for medulloblastomas (Fig. 2C). These medulloblastomas also showed high proliferative indices by Ki67 staining (Fig. 2D). The typical histologic characteristics are similar to what is observed in human medulloblastomas. These findings show that medulloblastoma formation can be initiated in BCCIP deficient mice. In contrast to BCCIP-CKD;p53<sup>LoxP/LoxP</sup> (*LoxPshBCCIP*<sup>+/-</sup>; p53<sup>LoxP/LoxP</sup>; *GFAP-Cre*<sup>+/-</sup>) mice, we did not observe medulloblastoma in BCCIP-CKD;p53<sup>LoxP/wt</sup> (*LoxPshBCCIP*<sup>+/-</sup>; p53<sup>LoxP/wt</sup>; *GFAP-Cre*<sup>+/-</sup>) mice (Fig. 2), indicating that complete loss-of-function of p53 is required for medulloblastoma formation in BCCIP-CKD mice (Table 1). Conditional p53 knockout alone did not induce medulloblastoma in the



Figure 1. p53 deficiency rescues microcephaly and neurologic defects of *BCCIP*-CKD mice. A, the average size of the brains (at age P21) from mice of six different genotypes (see Table 1 for details on genotypes). B, a set of representative brains among the BCCIP-CON and BCCIP-CKD mice combined with wild-type p53 ( $p53^{wt/wt}$ ), heterozygous p53 deletion ( $p53^{loxP/wt}$ ), or homozygous p53 deletion ( $p53^{loxP/loxP}$ ). C, a set of representative H&E staining histology of cerebrum and cerebellum at age P21. Neural markers: NeuN, Calbindin (D-28K), and GFAP.



BCCIP-CON; $p53^{LoxP/LoxP}$  ( $LoxPshBCCIP^{-/-}; p53^{LoxP/LoxP}; GFAP-Cre^{+/-}$ ) mice. This is consistent with a previous report (22).

However at older ages, a few BCCIP-CON; $p53^{LoxP/LoxP}$  ( $LoxPshBCCIP^{-/-}; p53^{LoxP/LoxP}; GFAP-Cre^{+/-}$ ) and BCCIP-CON; $p53^{LoxP/wt}$  ( $LoxPshBCCIP^{-/-}; p53^{wt/LoxP}; GFAP-Cre^{+/-}$ ) mice developed non-central nervous system (CNS) tumors (including sarcomas, lipomas, and lymphoid tumors), and the knockdown of *BCCIP* accelerated non-CNS tumor formation in p53 heterozygous mice, when comparing the survival of BCCIP-CKD; $p53^{LoxP/wt}$  ( $LoxPshBCCIP^{+/-}; p53^{LoxP/wt}; GFAP-Cre^{+/-}$ ) with that of BCCIP-CON; $p53^{LoxP/wt}$  ( $LoxPshBCCIP^{-/-}; p53^{LoxP/wt}; GFAP-Cre^{+/-}$ ;  $P = 0.004$ , *t*-test). The formation of non-CNS tumors may be due to basal levels of GFAP promoter activity in tissues other than CNS (23, 24). Together, findings shown in Fig. 2 strongly suggest that *BCCIP* knockdown resulted in a high prevalence of medulloblastoma tumorigenesis, revealing a tumor-suppressing role of *BCCIP*.

### The medulloblastomas formed in BCCIP-deficient mice have inactivation of the *Ptch1* gatekeeper tumor suppressor, and a wide range of alterations in the *Shh* pathway

Tumor suppressors can be classified as gatekeepers or caretakers (3), and they suppress tumorigenesis through distinct mechanisms. The gatekeeper tumor suppressors (such as RB, PTCH1, and PTEN,) often restrict cell proliferation, and a gatekeeper inactivation directly promotes tumor growth. Alternatively, the caretaker tumor suppressors do not directly control cell growth but maintain the genomic integrity. Caretaker deficiency causes stochastic genomic alterations that subsequently inactivate gatekeepers or activate oncogenes to cause tumor growth. Because *BCCIP* has been implicated in the maintenance of genomic integrity (5–8, 10), and *BCCIP* deficiency alone does not promote cell proliferation of neuronal progenitors in the external granule layer of the cerebellum (14), we speculated that compromised *BCCIP* may have caused secondary genetic alterations to inactivate certain gatekeeper

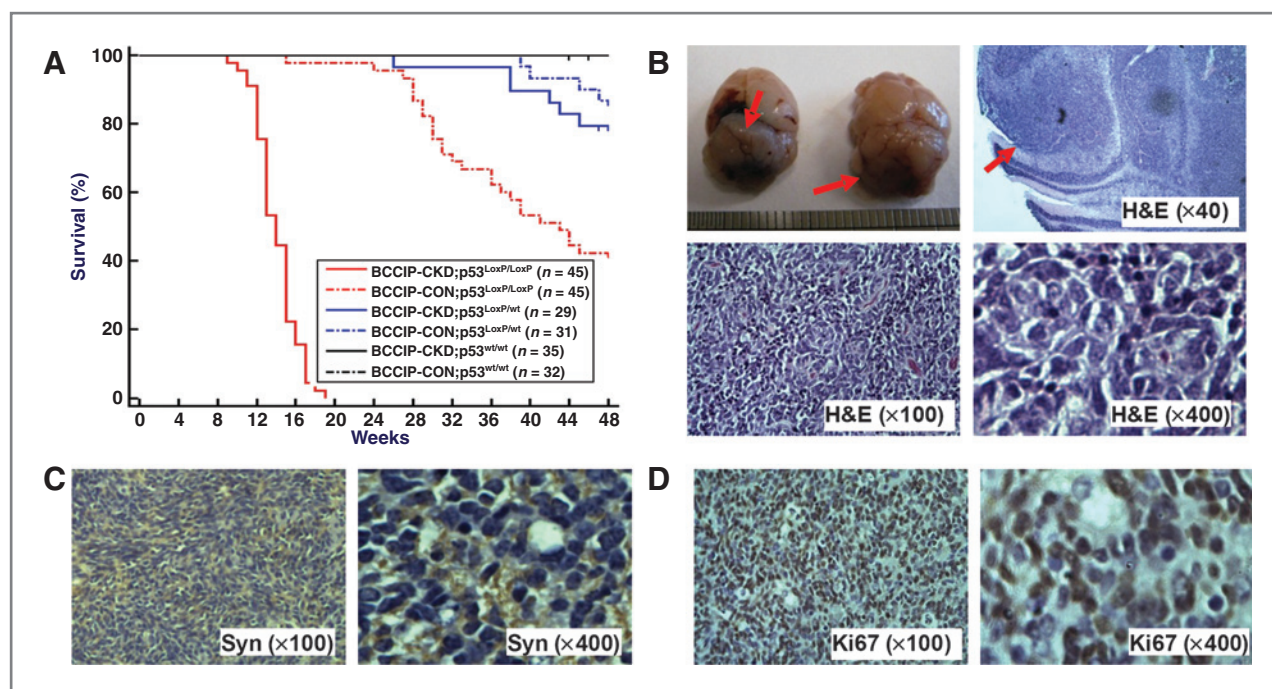


**Figure 2.** Medulloblastomas in conditional BCCIP knockdown and p53 knockout mice. The *LoxPshBCCIP* conditional BCCIP knockdown (BCCIP-CKD) mice were crossed with conditional p53 knockout (*p53<sup>LoxP/LoxP</sup>*) mice and then with the GFAP-Cre mice that expressed the Cre recombinase during embryogenesis. This resulted in mice with six different genotypes as shown in the inset of A and Table 1. These mice were observed for tumor formation for more than 48 months. A, survival curve of the mice. Medulloblastomas were formed in 100% of the BCCIP-CKD;*p53<sup>LoxP/LoxP</sup>* mice with an average onset of 95 days. None of the other mice developed medulloblastoma. Some of the BCCIP-CON;*p53<sup>LoxP/LoxP</sup>* mice were sacrificed due to growth of benign lipomas at older ages (see the text for details). B, the gross morphology of medulloblastoma formed in the BCCIP and p53-deficient BCCIP-CKD;*p53<sup>LoxP/LoxP</sup>* mice and H&E staining of the representative tumors. The top left panels show the medulloblastoma (indicated by arrows) from two mouse brains. The top right panel shows that the tumor foci are within the cerebellar external granule layer, with a typical histology of medulloblastoma. The bottom panels are H&E staining images of the tissues at the magnifications as indicated. C and D, immunohistochemical staining of the tumor tissue for synaptophysin (a medulloblastoma marker) and Ki67 (a proliferation marker).

genes, thus enabling medulloblastoma tumorigenesis. The Shh growth-signaling pathway is one of the major regulators of granule neuron progenitor cells during neurodevelopment. Shh signaling is normally suppressed by *PTCH1*, a gatekeeper gene that is often inactivated in human sporadic and hereditary medulloblastomas (25–27). In addition, Shh-mutated subtype tumors are thought to originate from the cerebellar external granule layer and have a tendency to be located away from the brainstem within the cerebellar hemispheres (28, 29). Coincidentally, we noticed the medulloblastomas that developed in BCCIP-CKD;*p53<sup>LoxP/LoxP</sup>* mice were mostly located in the external granular layer, away from the brainstem, and the embryonic external granular layer was the most BCCIP-deficient affected region as reported previously (14). Therefore, we analyzed the Shh status among medulloblastomas formed in BCCIP-CKD;*p53<sup>LoxP/LoxP</sup>* using nontumor cerebellar tissues from age-matched control mice. A critical negative regulator of the Shh pathway is the tumor-suppressor *Ptch1*, which suppresses smoothed (Smo)-dependent activation of Gli1 transcriptional activity (30–33). When *Ptch1* function is impaired, the Shh pathway is activated to promote cell growth. Using qPCR with primers covering the region of exons 17 and 18 of mouse *Ptch1*, we measured the expression of *Ptch1* in the tumors, and found a significant reduction of *Ptch1* expression in 16 of the 24 tested tumors (Fig. 4A). As expected, we were not

able to amplify the full-length *Ptch1* cDNA from the 16 cases. Among eight cases with apparent normal level of *Ptch1* mRNA based on qPCR of exons 17 and 18, we were able to amplify the approximately normal-sized *Ptch1* cDNA from six samples. Therefore, only six of the 24 cases have the expression of approximate full-length coding mRNA of *Ptch1*, and the other 18 cases likely had genetic alterations that prohibited the amplification of their cDNA. Furthermore, each of the amplified *Ptch1* cDNAs contained an inactivation mutation (Table 2) that was verified in the genomic DNA of the same tumor. In addition, it is striking that all mutations in the amplified cDNA were either deletions or insertions of multiple base pairs that resulted in truncation of *Ptch1*. We did not observe point mutations in these tumor samples (Table 2). These data suggest that *Ptch1* is a critical target for inactivation due to the genomic instability in the context of medulloblastoma formation after BCCIP knockdown. Thus, the majority of the tumors have lost *Ptch1*, and the remaining cases have deletions/insertions with multiple bases. These observations are consistent with a role of BCCIP in DNA double-strand break repair, including homologous recombination (5, 6).

In the Shh pathway, the critical downstream target of *Ptch1* is Smo, which controls the expression of Gli1, Atoh1, N-Myc, and D-cyclins. These downstream elements are known to be

**Table 2.** Altered sequence of *Ptch1* cDNA in medulloblastomas

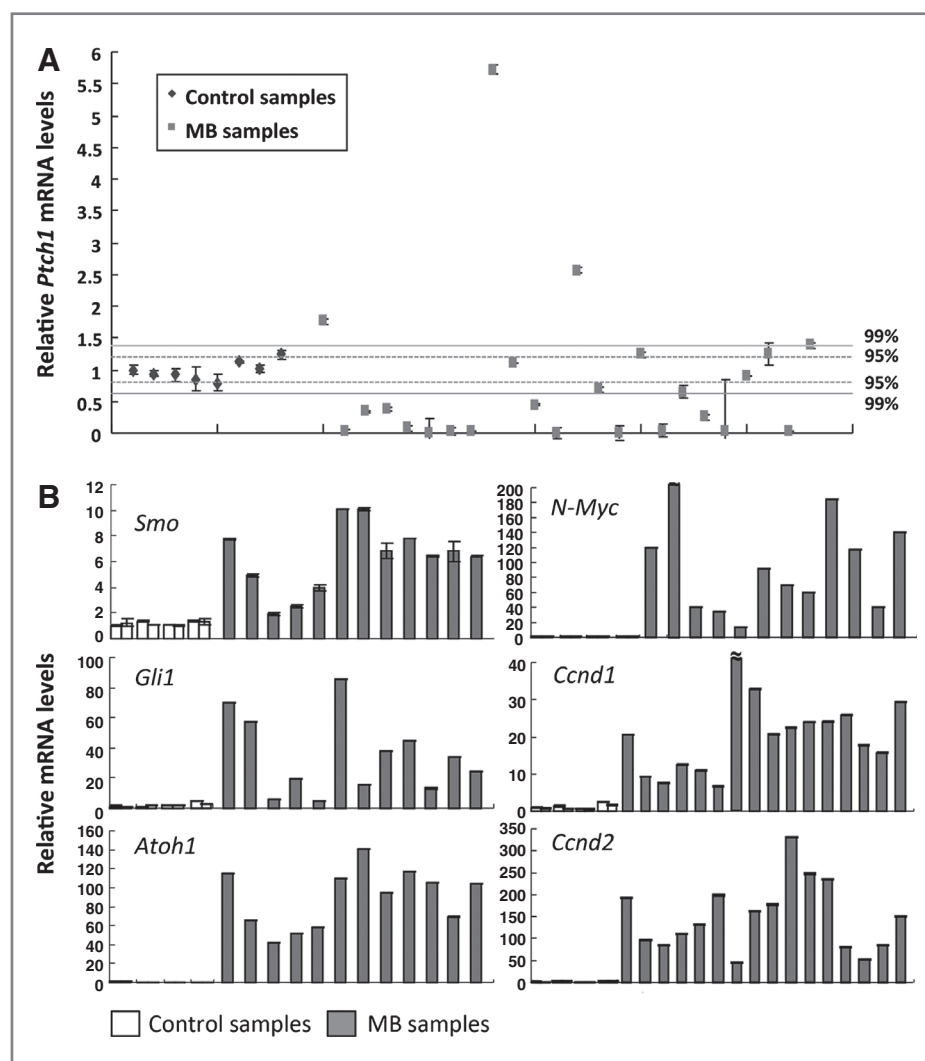
Tumor ID	<i>Ptch1</i> mutations	Altered sequences <sup>a</sup>
MB20	14nt duplication in exon 10	CTGGCTGGCGTCTCTGTTGGTTGCGTCTCTGTTGGTTGCGCTGTCAGTGG
MB36	14nt deletion in exon 16	CAGACTGGCA (GCCGAGACAAGCCC)ATCGACATTA
MB59	4nt deletion in exon 10	GTCCTGTTGG (TTGC) GCTGTCAGTG
MB73	14nt duplication in exon 10	CTGGCTGGCGTCTCTGTTGGTTGCGTCTCTGTTGGTTGCGCTGTCAGTGG
MB79	7nt deletion in exon 18	CCTACGAGAC (ACCTCAG)ACTTTGTGGA
MB89	Deletion: 3nt of exon 11, Intron-11, and 123nt of exon 12.	ATTCCATTG (AGG-Intron 11-ACAGGACTGGGGAGTGCCTCAAGCGCACCGGAGCC- AGCGTGGCCCTCACCTCCATCAGCAATGTCACCGCCTTCTTCATGGCCGCATTGA- TCCCTATCCCTGCCCTGCGAGCGTCTCCCTCC)AGGCTGCTGT

<sup>a</sup>Parentthesized sequences are the deleted segments in tumor; underlined sequences are the duplicated segments.

critical regulators of granule neuron progenitors (34–37), which are the originators of medulloblastoma. Along with the *Ptch1* mutations and loss of *Ptch1* expression, we observed high levels of *Smo*, *Gli1*, *Atoh1*, *N-Myc*, and *D-cyclins* in the medulloblastomas compared with controls (Fig. 3B; Supplementary

Table S4). Together, these data suggest that the initial BCCIP knockdown had triggered the inactivation of the *Ptch1* gate-keeper tumor suppressor and caused widespread alterations, leading to the activation of the Shh signaling pathway, which is known to promote medulloblastoma formation.

**Figure 3.** Dysregulation of the Shh signaling pathway in medulloblastomas. The qPCR analyses were used to measure the relative level of mRNA in medulloblastoma tissues derived from BCCIP-CKD;p53<sup>LoxP/LoxP</sup> mice. The mRNA levels of age-matched control (3-month-old) cerebellums were also measured. A, relative level of *Ptch1* mRNA in 24 medulloblastoma samples. Control samples are (from left to right): BCCIP-CON (*LoxPshBCCIP*<sup>+/-</sup>; p53<sup>wt/wt</sup>; GFAP-Cre<sup>-/-</sup>; first 2 control data points from the left, n = 2), BCCIP-CKD (*LoxPshBCCIP*<sup>+/-</sup>; p53<sup>wt/wt</sup>; GFAP-Cre<sup>+/-</sup>; control data points 3 and 4 from the left, n = 2), GFAP-Cre (*LoxPshBCCIP*<sup>+/-</sup>; p53<sup>wt/wt</sup>; GFAP-Cre<sup>+/-</sup>; n = 2) and BCCIP-CON;p53<sup>LoxP/LoxP</sup> (*LoxPshBCCIP*<sup>-/-</sup>; p53<sup>LoxP/LoxP</sup>; GFAP-Cre<sup>+/-</sup>; n = 2). The mean and SD of *Ptch1* mRNA level were calculated from control samples. On the basis of the normal distribution, the 95% confidence limit ( $P < 0.05$ ) was set at 1.96-fold of the SD, and the 99% confidence limit ( $P < 0.01$ ) was set at 2.58-fold of the SD. The 95% and 99% confidence ranges are marked in the graph. A total of 16 cases displayed reduction of *Ptch1* mRNA levels. B, the wide range of mRNA upregulation of key components of the Shh pathway as indicated in the specific panels. A total of 12 MB samples were analyzed in *Smo*, *Gli1*, *Atoh1*, *N-Myc*, and 16 MB samples were analyzed in *Ccnd1* and *Ccnd2*.





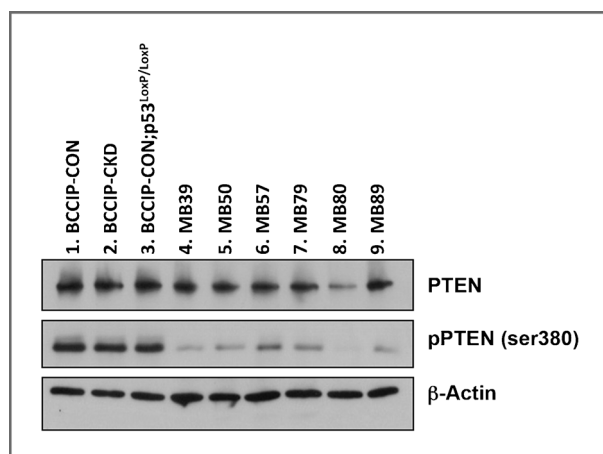


Figure 4. PTEN expression in in medulloblastomas. Western blots were performed to measure the levels of PTEN and pPTEN-ser380 in the medulloblastomas (lanes 4–9). As the controls, proteins were extracted from the cerebellums of *BCCIP-CON* (*LoxPshBCCIP*<sup>-/-</sup>; *p53*<sup>w<sup>t</sup>/w<sup>t</sup></sup>; *GFAP-Cre*<sup>+/-</sup>), *BCCIP-CKD* (*LoxPshBCCIP*<sup>+/-</sup>; *p53*<sup>w<sup>t</sup>/w<sup>t</sup></sup>; *GFAP-Cre*<sup>+/-</sup>), *BCCIP-CON;p53*<sup>LoxP/LoxP</sup> (*LoxPshBCCIP*<sup>-/-</sup>; *p53*<sup>LoxP/LoxP</sup>; *GFAPCre*<sup>+/-</sup>) mice that were 3 months old (lanes 1–3).

#### PTEN status in medulloblastoma induced by BCCIP deficiency

Because the gatekeeper PTEN has been implicated in brain tumors including medulloblastoma (38; 39, 40), we investigated whether there is a genetic changes on PTEN. However, we did not find evidence of PTEN mRNA reduction, or mutations in the PTEN coding-region cDNA. Western blot analysis revealed relatively normal expression level of PTEN protein within most of the tumor tissues (Fig. 4). Thus, PTEN inactivation seems to be an unlikely cause of the tumors obtained from the BCCIP conditional knockdown mice. However, we observed a reduced PTEN Ser-380 phosphorylation compared with control tissues (Fig. 4). Although it had been suggested that C-terminal phosphorylation of PTEN may regulate its stability (41, 42), we did not observe an altered PTEN protein levels in the tumor tissues as shown in Fig. 4. The significance of the reduced PTEN c-terminal phosphorylation in the tumor tissues remains to be determined.

#### Restored BCCIP expression in medulloblastomas

In our mouse model, *BCCIP* expression was conditionally knocked down by GFAP-mediated Cre expression during embryogenesis, which differs from the classical knockout approach. First, the knockout approach would completely abolish the expression of wild-type *BCCIP*; the knockdown approach is unlikely to do so, leaving a reduced *BCCIP* expression. Second, the knockout approach permanently deletes the endogenous *BCCIP* allele and *BCCIP* expression cannot be restored during the later stages of tumor progression. Conversely, the knockdown approach leaves the endogenous *BCCIP* locus intact and there is a possibility to restore *BCCIP* expression. To examine *BCCIP* expression in the tumor tissues, we measured BCCIP protein levels in the medulloblastomas and that of age-matched (3-month-old) control cerebellums (*BCCIP-CON*, *BCCIP-CKD*, *GFAP-Cre*, and *BCCIP-CON*;

*p53*<sup>LoxP/LoxP</sup> mice). To our surprise, a restored expression of BCCIP protein among all tumor samples was observed (Fig. 5A). We further compared BCCIP levels of the tumor regions (Cb-T) with the tumor-neighboring cerebellum region (Cb-NT) that may contain both tumor and normal cells, and the cortex nontumor (Cx) region from the same animal. Again, the BCCIP expression detected in tumor tissues was significantly higher than in nontumor tissues among all measured 24 samples (see Fig. 5B for three representative cases). As expected, the downregulation of p53 expression was observed in the tumor tissues (Fig. 5B), and all tumor tissues displayed higher expression levels of PCNA, a proliferation marker (Fig. 5B). As expected, the normal tissue have detectable level of p53 (Fig. 5B), due to the presence of GFAP-negative cells in the normal tissues. A small and reduced level of p53 can be detected in the tumor tissue (Fig. 5B, lanes 2, 5, and 8), and is likely contributed by mixed normal cells in the tumor tissues.

We used qPCR measurements to confirm elevated levels of BCCIP in medulloblastomas (Fig. 5C). These data confirmed that *BCCIP* expression was restored in the tumor tissues. Although the BCCIP-CKD mouse brains were reported to have lower level of BCCIP expression during embryogenesis at newborn age than non-knockdown mice (14), we noticed a minimum reduction of protein level in the whole brain at the age of 3 months (compare lane 2 of Fig. 5A with that of lane 1, and control data points 3 and 4 with the rest of the control data points in Fig. 5C). This is due to the conditional nature of our GFAP-Cre system that only targets the GFAP-positive cells for BCCIP silencing. During embryogenesis and at the newborn stage, GFAP is expressed in multipurpose progenitor cells, and these cells constitute a major portion of brain tissue. Thus, a clear BCCIP down regulation can be verified among embryo E15.5 neurospheres and newborn (P1) brain tissues as reported previously (14). However, at the time of medulloblastoma development (3 months), GFAP is mainly expressed in astrocytes, which are no longer a major portion in the brain tissues. When the 3-month-old brain tissue is used to measure BCCIP level, it cannot reflect the BCCIP knockdown status in the GFAP-positive cell population.

To identify the cause of the restored BCCIP expression in the tumor tissues that originally possessed the BCCIP shRNA expression cassette, we analyzed the status of the BCCIP shRNA cassette among the genomic DNA from the tumor tissues. Interestingly, we found that all of the analyzed tumor samples had lost the transgenic BCCIP shRNA expression cassette *LoxPshBCCIP*, whereas they maintained the deleted p53 alleles and the GFAP-Cre cassette (see Fig. 5D for three representative cases). Therefore, it seems that the tumors have found a way to restore BCCIP expression by deleting the BCCIP shRNA expression cassette, likely by growth pressure of the tumor cells. No *BCCIP* mutation was identified from the tumor tissues analyzed.

These surprising findings imply that the expression of *BCCIP* is required for the continued growth or progression of medulloblastomas. The genomic instability generated by the initial and transient *BCCIP* downregulation was sufficient to cause oncogenic transformation due to a stochastic activation of progrowth Shh signaling (Figs. 3 and 4). Furthermore, the

proliferative tumor cells have even higher level of BCCIP RNA and proteins than normal tissue, implying a role of BCCIP in promoting tumor progression, which is consistent with the essential function of BCCIP in cell growth.

## Discussion

### **BCCIP represents a class of tumorigenesis modulators that function as suppressor of initiation but a requisite for progression**

In this study, we have shown that conditional BCCIP knockdown contributes to the development of medulloblastomas. On the basis of the functions of BCCIP in DNA repair, cell-cycle regulation, and mitosis (5–7, 10, 11), it is conceivable that BCCIP functions as a caretaker tumor-suppressor gene. Reduced BCCIP function is expected to cause genomic instability that can inactivate gatekeeper tumor suppressors, which is consistent with the observed alterations in the gatekeeper pathways (i.e., Shh) and the high penetrance of medulloblastomas in the BCCIP-CKD;p53<sup>LoxP/LoxP</sup> mice (Table 1, Fig. 2). These data strongly suggest that BCCIP has a tumor-suppression responsibility. However, it was paradoxical that BCCIP expression was restored and expressed at even higher levels in the fully developed tumors (Fig. 5), which implies a possible tumor promoter role for BCCIP. As a consolidated model, we propose that the initial BCCIP deficiency (caused by BCCIP shRNA expression) elicited stochastic genomic instability that eventually compromised the function of gatekeepers in the Shh pathway. When the progrowth pathways were activated, they were autonomous in supporting cell growth, which caused oncogenic transformation of the neural progenitor cells. At this stage, BCCIP deficiency is no longer needed to trigger transformation and becomes an obstacle for the progression of the transformed cells, due to *BCCIP*'s functions for DNA replication, DNA repair, and mitosis. In the context of tumor progression, the sustained rapid proliferation favors those cells with spontaneous deletion of the BCCIP knockdown cassette. Thus, during tumor progression, when gatekeeper functions of *Ptch1* have been inactivated, *BCCIP* become essential for a sustained growth of the tumor. This mode of action underscores the paradoxical roles of BCCIP in tumorigenesis. We postulate that BCCIP represents a unique class of modulators of tumorigenesis that are Suppressors of Initiation but Requisite for Progression (SIRP).

We further suggest that BCCIP exhibits a typical mode of action for essential caretaker genes in tumorigenesis. On one hand, a transient or subtle downregulation of these genes is sufficient to trigger genomic instability, leading to oncogenic transformations from autonomous proproliferation signaling networks. On the other hand, the sustained growth of transformed cells demands the availability of the same genes due to their essential roles in cell division and proliferation. Unlike the classical tumor suppressors that are often found mutated in the tumor tissue, the SIRP types of genes regulate tumorigenesis in an unconventional way. It only takes a transient or subtle dysfunction to trigger the oncogenic transformations, and their deficiencies work in a "hit-and-run" manner to initiate tumor-

igenesis. Thus, inactivation mutations in the SIRP genes may be rare in fully developed tumors, and a transient and epigenetic downregulation of SIRP genes may be more prevalent in conferring tumorigenesis. This scenario may help explaining how some epigenetically regulated tumor suppressors play a role in tumorigenesis. It further raises several critical questions when considering the roles of DNA repair genes in tumorigenesis. First, do essential DNA repair genes typically function as conventional tumor suppressors? Second, are there any other DNA repair genes that possess SIRP roles in tumorigenesis? Lastly, what environmental factors play a role in the transient dysregulation of the SIRP genes to promote tumorigenesis?

### **Conditional knockdown as an ideal approach to identify genes with paradoxical functions at different stages of tumorigenesis**

As a gene involved in genomic integrity, *BCCIP* is unlikely to be the only gene with the paradoxical SIRP functions. The conventional knockout approach is unlikely to reveal the SIRP genes with multiple and, often, opposing roles at different stages of tumorigenesis. As discussed in a previous report (7), we initially opted to use the conditional knockdown approach to minimize the possibility of interference by BCCIP deletion on its overlapping genes. This approach leaves the endogenous BCCIP locus intact. When BCCIP is indeed critical for tumor progression, the growth pressure of transformed cells would favor cells with a spontaneous deletion of the BCCIP knockdown cassette. In addition, this approach downregulates, but does not mutate or abolish *BCCIP* and has advantages over the conventional knockout approach as it can faithfully reproduce situations where gene downregulation, but not mutation, contributes to tumorigenesis. In contrast, a conventional knockout strategy would permanently delete the gene(s) of interest. The absence of essential functions of the gene(s) would prevent tumor progression and, thus, development of advanced tumors would be unlikely. We were fortunate to observe such a unique SIRP role of BCCIP in tumorigenesis because we opted to use a conditional knockdown approach.

### **Distinct features of the BCCIP knockdown medulloblastomas mouse model**

Although p53 deletion alone in the GFAP-Cre- or Nestin-Cre-based conditional knockout mice is not sufficient to cause medulloblastoma in many DNA repair-deficient mouse models (this study and another; see ref. 22), p53 deficiency combined with DSB repair defects (including NHEJ and HR) and DNA damage signaling can induce medulloblastoma (43). It has been shown that Nestin-Cre-mediated conditional knockout of BRCA2 and NBS1 also caused medulloblastomas (44, 45). In these mouse models, the Nestin promoter becomes active at around embryonic day 11 (E11), primarily in the CNS and peripheral nervous system during embryogenesis (46). In our study, we crossed FVB-*LoxPshBCCIP*<sup>+/+</sup> mice with FVB-*Tg* (*GFAP-Cre*) transgenic mice that express Cre recombinase under the control of the human GFAP promoter. Although only glial cells are immune-reactive for GFAP in adult brain, embryonic GFAP-promoter activity is not restricted to glial



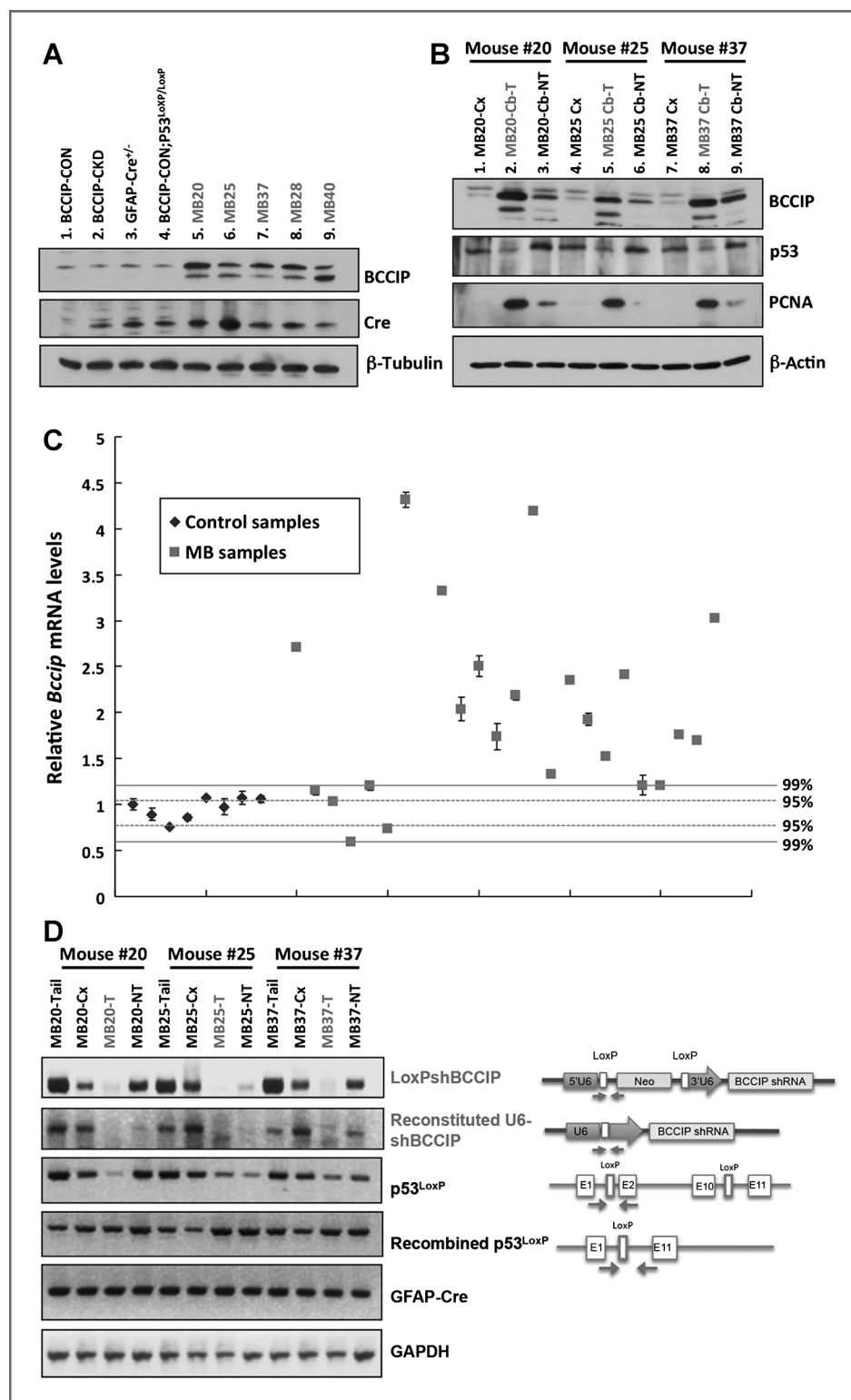


Figure 5. BCCIP expression in the medulloblastoma formed from the BCCIP-knockdown mice. Proteins and DNA from tumor tissues (Cb-T), tumor-bordering cerebellum (Cb-NT), and nontumor cortex (Cx) were subjected to Western blot and PCR genotype analyses. A, the BCCIP and Cre protein levels. It reveals an upregulation of BCCIP in medulloblastoma tissues (lanes 5–9) compared with the cerebellums from BCCIP-CON (*LoxPshBCCIP*<sup>+/-</sup>; *p53*<sup>wt/wt</sup>; *GFAP-Cre*<sup>-/-</sup>; lane 1), BCCIP-CKD (*LoxPshBCCIP*<sup>+/-</sup>; *p53*<sup>wt/wt</sup>; *GFAP-Cre*<sup>+/-</sup>; lane 2), GFAP-Cre (*LoxPshBCCIP*<sup>-/-</sup>; *p53*<sup>wt/wt</sup>; *GFAP-Cre*<sup>+/-</sup>; lane 3), and BCCIP-CON;p53<sup>LoxP/LoxP</sup> (*LoxPshBCCIP*<sup>-/-</sup>; *p53*<sup>LoxP/LoxP</sup>; *GFAP-Cre*<sup>+/-</sup>; lane 4) mice. B, the BCCIP, p53, and PCNA protein expression level in three representative mice, MB-20, 25, and 37. (Continued on the following page.)

progenitor cells. Much like Nestin-Cre, GFAP-promoter is active in multipotent stem cells, including neural progenitor cells during embryogenesis with a peak activity at around embryonic day 13.5 (E13.5) (21). However, there is a difference between the two transgenic mouse strains. Nestin-Cre mice express Cre recombinase in common neural progenitors mostly during embryogenesis, whereas hGFAP-Cre transgenic mice express Cre recombinase in both embryonic common progenitor cells as well as in adult glial cells (21).

The conditional homozygous BRCA2 deletion in *Brca2<sup>Nestin-cre</sup>* mice resulted in neural development defects and medulloblastoma when p53 was also deleted (44). As a BRCA2 interacting protein, BCCIP has been shown to play a role in homologous recombination, cell-cycle regulation, and chromosome stability (5, 6, 8). Although certain features such as viable mice with no tumor formation in *BCCIP* or *BRCA2* deficiency alone are similar, additional characteristics of the BCCIP-CKD mice make it distinguishable from the BRCA2 knockout mice. First, homozygous p53 deletion almost completely rescued microcephaly in BCCIP-CKD mice (Fig. 1), but it only partially rescued the microcephaly in BRCA2 knockout mice (44). Second, when both copies of the p53 gene were deleted, all of the BCCIP-CKD mice developed medulloblastoma, but only 83% of the BRCA2 knockout mice developed tumors with a similar onset of approximately 3 months (44). Lastly, none of the BCCIP-CKD mice with p53 heterozygosity developed tumors; however, 72% of the BRCA2 conditional knockout mice with p53 heterozygosity developed medulloblastoma with a concurrent loss of the second copy of the p53 in the tumor cells (44). This is a drop from 83% (p53 homozygous) to 72% (p53 heterozygous) in BRCA2 knockout mice, compared with 100% (p53 homozygous) to 0% (p53 heterozygous) for BCCIP knockdown mice. It implies that BCCIP-deficiency-induced medulloblastoma is more dependent on complete loss of p53 function than BRCA2 knockout. However, it was noted that the BRCA2 study used the constitutive p53-deficient mice rather than a conditional p53 *LoxP* mice (44).

*Nbs1* is another gene involved in DNA damage response. The *Nbs1<sup>Nestin-Cre</sup>* conditional knockout mice had severe neural degeneration, ataxia, and microcephaly to a similar extent as our BCCIP-CKD mice (45). In addition, p53 deletion remarkably rescued the microcephaly and neural degeneration phenotype of *NBS1<sup>Nestin-Cre</sup>* knockout mice as with BCCIP-CKD

mice. However, unlike in BCCIP-CKD mice, p53 deletion did not promote tumor formation in *NBS1<sup>Nestin-cre</sup>* mice (45). These distinct features suggest that BCCIP's roles in neurodevelopment and medulloblastoma formation may be independent of *NBS1* and *BRCA2*. However, it is possible that *NBS1* may be another essential gene with SIRP function, and irreversible *NBS1* deficiency (in the knockout mouse model) may have had prevented the transformed progenitor cells from a sustained progression into medulloblastomas.

#### Activation of the Shh pathway in medulloblastoma in BCCIP-deficient mice

Medulloblastoma is the most common childhood malignant brain tumor. This type of tumor originates from granular neural progenitors in the cerebellum (47). On the basis of gene expression profiling, different subtypes of human medulloblastomas are characterized by alterations of multiple cell-growth signaling pathways, including the Shh, Wnt, and the Notch signaling (27, 48–50). More than 25% of sporadic human medulloblastomas have mutations in key components of the Shh signaling pathway, such as *Ptch1* and *Smo* (33, 48). Interestingly, all of the medulloblastomas developed in the BCCIP-CKD; *p53<sup>LoxP/LoxP</sup>* mice had abnormalities in at least one, and often multiple, component of the Shh pathway (Fig. 3; Supplementary Table S4). A striking feature of *Ptch1* mutations from our BCCIP knockdown mice is that the majority of the tumors have lost the *Ptch1* gene (18/24), and the remaining mutations (6/24) involve large deletions or duplication of normal sequences in the *Ptch1* gene but do not involve single base-pair mutations. This feature indicates that BCCIP-deficiency-induced *Ptch1* mutations are likely due to DNA repair mechanisms involved in large rearrangements of DNA fragments, which is consistent with BCCIP's role in DNA double-strand break repair and replication slippage.

#### PTEN status in medulloblastoma

Reduced PTEN expression was shown in human medulloblastomas (39). In addition, frequent loss of heterozygosity of chromosome 10q, where PTEN is located (10q23.31), was observed in human medulloblastomas (40). Although reduced expression levels of PTEN were observed in a small fraction of tumors (1 out of 9 as shown in Fig. 4), we did not detect mutations in the *Pten* ORF region (Fig. 4). Interestingly, we observed a

(Continued.) Lanes 2, 5, and 8 are the medulloblastoma tissues (Cb-T); lanes 3, 6, and 9 are tissues from tumor-bordering regions of the cerebellums (Cb-NT); and lanes 1, 4, and 7 are the tissues of cerebral cortex (Cx) of the same mice. Upregulation of BCCIP protein and downregulation of p53 levels were detected in medulloblastoma tissues (Cb-T; lanes 2, 5, and 8). C, the relative mRNA levels of BCCIP in medulloblastoma using GAPDH as an internal control. Control samples are age-matched (3-month-old) cerebellums of BCCIP-CON (*LoxPshBCCIP<sup>+/-</sup>*; *p53<sup>wt/wt</sup>*; *GFAP-Cre<sup>-/-</sup>*; first two control data points from the left, *n* = 2), BCCIP-CKD (*LoxPshBCCIP<sup>+/-</sup>*; *p53<sup>wt/wt</sup>*; *GFAP-Cre<sup>+/-</sup>*; control data points 3 and 4 from the left, *n* = 2), *GFAP-Cre* (*LoxPshBCCIP<sup>-/-</sup>*; *p53<sup>wt/wt</sup>*; *GFAP-Cre<sup>+/-</sup>*; *n* = 2), and BCCIP-CON; *p53<sup>LoxP/LoxP</sup>* (*LoxPshBCCIP<sup>-/-</sup>*; *p53<sup>LoxP/LoxP</sup>*; *GFAP-Cre<sup>+/-</sup>*; *n* = 2). Mean and SD of the BCCIP mRNA level were calculated from control samples. On the basis of the normal distribution, the 95% confidence limit (*P* < 0.05) was set at 1.96-fold of the SD, and the 99% confidence limit (*P* < 0.01) was set at 2.58-fold of the SD. The 95% and 99% confidence ranges are marked in C. Sixteen medulloblastoma samples showed reduction of BCCIP mRNA levels. D, loss of the BCCIP shRNA expression cassette in the medulloblastomas. Shown here are representative PCR genotyping results for the DNA extracted from medulloblastoma tissues (MB-T), tails (MB-Tail), nontumor cortex (MB-Cx), and nontumor cerebellums (MB-NT) from three mice. Panel 1 shows the detection of the split U6 promoter *LoxPshBCCIP*. Panel 2 detects the reconstituted U6-shBCCIP cassette after Cre-mediated recombination. Panel 3 detects the floxed p53 allele (and the wild-type p53 allele, lower band). Panel 4 detects the p53 allele after Cre-mediated *LoxP* recombination. Panel 5 shows the presence of *GFAP-Cre* transgenes in the tissues. GAPDH was used as a PCR control (panel 6). The genotype structure and approximate primer locations for PCR genotype for panels 1–4 are shown on the right side of each panel. As shown here, all medulloblastoma tissues (MB-T) lost the BCCIP shRNA expression cassette, although they all carry the *GFAPCre* cassette and recombined p53 allele.

reduced PTEN phosphorylation at Ser380 in the tumor tissues (Fig. 4). The significance of this observation remains to be investigated.

In summary, our study showed that, due to BCCIP's roles in the maintenance of genomic integrity, conditional BCCIP deficiency synergizes with loss of p53 to promote medulloblastoma. This suggests a tumor-suppressor role for BCCIP. However, BCCIP is also required for tumor progression. These observations revealed a paradoxical class of modulators of tumorigenesis that act as SIRPs. We further propose that only a transient downregulation, but not necessarily a permanent mutation, of a SIRP is sufficient to confer tumorigenesis. This concept has major implications on how dynamic regulation of essential caretaker genes, such as by epigenetic mechanisms of regulation, can contribute to tumorigenesis.

#### Disclosure of Potential Conflicts of Interest

No potential conflicts of interest were disclosed.

#### Authors' Contributions

**Conception and design:** Y-Y. Huang, Z. Shen

**Development of methodology:** Y-Y. Huang, L. Dai, J. Liu, Z. Shen  
**Acquisition of data (provided animals, acquired and managed patients, provided facilities, etc.):** L. Dai, H. Lu, Z. Shen  
**Analysis and interpretation of data (e.g., statistical analysis, biostatistics, computational analysis):** Y-Y. Huang, D. Gaines, Z. Shen  
**Writing, review, and/or revision of the manuscript:** Y-Y. Huang, D. Gaines, R. Droz-Rosario, J. Liu, Z. Shen  
**Administrative, technical, or material support (i.e., reporting or organizing data, constructing databases):** Y-Y. Huang, H. Lu, J. Liu, Z. Shen  
**Study supervision:** Z. Shen

#### Acknowledgments

The authors thank Dr. W. Hu (Rutgers Cancer Institute of New Jersey) for suggestions on qPCR analysis.

#### Grant Support

This work was financially supported by the NIH (grant no. R01CA156706 to Z. Shen) and the Transgenic and Knockout Mouse and the Histopathology and Imaging shared resources of the Rutgers Cancer Institute of New Jersey (P30CA072720).

The costs of publication of this article were defrayed in part by the payment of page charges. This article must therefore be hereby marked *advertisement* in accordance with 18 U.S.C. Section 1734 solely to indicate this fact.

Received June 23, 2013; revised September 20, 2013; accepted September 26, 2013; published OnlineFirst October 21, 2013.

#### References

- Hanahan D, Weinberg RA. Hallmarks of cancer: the next generation. *Cell* 2011;144:646-74.
- Shen Z. Genomic instability and cancer: an introduction. *J Mol Cell Biol*. 2011;3:1-3.
- Kinzler KW, Vogelstein B. Cancer-susceptibility genes. Gatekeepers and caretakers. *Nature* 1997;386:761, 763.
- Liu J, Yuan Y, Huan J, Shen Z. Inhibition of breast and brain cancer cell growth by BCCIPalpha, an evolutionarily conserved nuclear protein that interacts with BRCA2. *Oncogene* 2001;20:336-45.
- Lu H, et al. The BRCA2-interacting protein BCCIP functions in RAD51 and BRCA2 focus formation and homologous recombinational repair. *Mol Cell Biol* 2005;25:1949-57.
- Lu H, Yue J, Meng X, Nickloff JA, Shen Z. BCCIP regulates homologous recombination by distinct domains and suppresses spontaneous DNA damage. *Nucleic Acids Res* 2007;35:7160-70.
- Lu H, et al. Essential roles of BCCIP in mouse embryonic development and structural stability of chromosomes. *PLoS Genet* 2011;7:e1002291.
- Meng X, Fan J, Shen Z. Roles of BCCIP in chromosome stability and cytokinesis. *Oncogene* 2007;26:6253-60.
- Meng X, Liu J, Shen Z. Genomic structure of the human BCCIP gene and its expression in cancer. *Gene* 2003;302:139-46.
- Meng X, Liu J, Shen Z. Inhibition of G1 to S cell cycle progression by BCCIP beta. *Cell Cycle* 2004;3:343-8.
- Meng X, Lu H, Shen Z. BCCIP functions through p53 to regulate the expression of p21Waf1/Cip1. *Cell Cycle* 2004;3:1457-62.
- Meng X, Yue J, Liu Z, Shen Z. Abrogation of the transactivation activity of p53 by BCCIP down-regulation. *J Biol Chem* 2007;282:1570-6.
- Fan J, Wray J, Meng X, Shen Z. BCCIP is required for the nuclear localization of the p21 protein. *Cell Cycle* 2009;8:3019-24.
- Huang YY, Lu H, Liu S, Droz-Rosario R, Shen Z. Requirement of mouse BCCIP for neural development and progenitor proliferation. *PLoS ONE* 2012;7:e30638.
- Mao N, Zhou Q, Kojic M, Perez-Martin J, Holloman WK. Ortholog of BRCA2-interacting protein BCCIP controls morphogenetic responses during DNA replication stress in *Ustilago maydis*. *DNA Repair (Amst)* 2007;6:1651-60.
- Liu J, Lu H, Ohgaki H, Merlo A, Shen Z. Alterations of BCCIP, a BRCA2 interacting protein, in astrocytomas. *BMC Cancer* 2009;9:268.
- Roversi G, et al. Identification of novel genomic markers related to progression to glioblastoma through genomic profiling of 25 primary glioma cell lines. *Oncogene* 2006;25:1571-83.
- Rewari A, et al. BCCIP as a prognostic marker for radiotherapy of laryngeal cancer. *Radiother Oncol* 2009;90:183-8.
- Lee Y, et al. Patched2 modulates tumorigenesis in patched1 heterozygous mice. *Cancer Res* 2006;66:6964-71.
- Marino S, Vooijs M, van Der Gulden H, Jonkers J, Berns A. Induction of medulloblastomas in p53-null mutant mice by somatic inactivation of Rb in the external granular layer cells of the cerebellum. *Genes Dev* 2000;14:994-1004.
- Zhuo L, et al. hGFAP-cre transgenic mice for manipulation of glial and neuronal function in vivo. *Genesis* 2001;31:85-94.
- Frappart PO, et al. Recurrent genomic alterations characterize medulloblastoma arising from DNA double-strand break repair deficiency. *Proc Natl Acad Sci USA* 2009;106:1880-5.
- Brenner M, Kisseberth WC, Su Y, Besnard F, Messing A. GFAP promoter directs astrocyte-specific expression in transgenic mice. *J Neurosci* 1994;14:1030-7.
- Brenner M. Structure and transcriptional regulation of the GFAP gene. *Brain Pathol* 1994;4:245-57.
- Wechsler-Reya R, Scott MP. The developmental biology of brain tumors. *Annu Rev Neurosci* 2001;24:385-428.
- Zindy F, et al. Genetic alterations in mouse medulloblastomas and generation of tumors de novo from primary cerebellar granule neuron precursors. *Cancer Res* 2007;67:2676-84.
- Gilbertson RJ, Ellison DW. The origins of medulloblastoma subtypes. *Annu Rev Pathol* 2008;3:341-65.
- Marino S. Medulloblastoma: developmental mechanisms out of control. *Trends Mol Med* 2005;11:17-22.
- Gibson P, et al. Subtypes of medulloblastoma have distinct developmental origins. *Nature* 2010;468:1095-9.
- Stecca B, Ruiz i Altaba A. Brain as a paradigm of organ growth: Hedgehog-Gli signaling in neural stem cells and brain tumors. *J Neurobiol* 2005;64:476-90.
- Dellovade T, Romer JT, Curran T, Rubin LL. The hedgehog pathway and neurological disorders. *Annu Rev Neurosci* 2006;29:539-63.
- Ruiz i Altaba A, Palma V, Dahmane N. Hedgehog-Gli signalling and the growth of the brain. *Nat Rev Neurosci* 2002;3:24-33.
- Zurawel RH, et al. Analysis of PTCH/SMO/SHH pathway genes in medulloblastoma. *Genes Chromosomes Cancer* 2000;27:44-51.



34. Kenney AM, Cole MD, Rowitch DH. Nmyc upregulation by sonic hedgehog signaling promotes proliferation in developing cerebellar granule neuron precursors. *Development* 2003;130:15–28.
35. Huard JM, Forster CC, Carter ML, Sicinski P, Ross ME. Cerebellar histogenesis is disturbed in mice lacking cyclin D2. *Development* 1999;126:1927–35.
36. Pogoriler J, Millen K, Utset M, Du W. Loss of cyclin D1 impairs cerebellar development and suppresses medulloblastoma formation. *Development* 2006;133:3929–37.
37. Lee Y, et al. A molecular fingerprint for medulloblastoma. *Cancer Res* 2003;63:5428–37.
38. Castellino RC, et al. Heterozygosity for Pten promotes tumorigenesis in a mouse model of medulloblastoma. *PLoS One* 2010;5:e10849.
39. Hartmann W, et al. Phosphatidylinositol 3'-kinase/AKT signaling is activated in medulloblastoma cell proliferation and is associated with reduced expression of PTEN. *Clin Cancer Res* 2006;12:3019–27.
40. Griffin CA, Hawkins AL, Packer RJ, Rorke LB, Emanuel BS. Chromosome abnormalities in pediatric brain tumors. *Cancer Res* 1988;48:175–80.
41. Vazquez F, Ramaswamy S, Nakamura N, Sellers WR. Phosphorylation of the PTEN tail regulates protein stability and function. *Mol Cell Biol* 2000;20:5010–8.
42. Yang Z, et al. Reduced expression of PTEN and increased PTEN phosphorylation at residue Ser380 in gastric cancer tissues: a novel mechanism of PTEN inactivation. *Clin Res Hepatol Gastroenterol* 2013;37:72–9.
43. Frappart PO, McKinnon PJ. Mouse models of DNA double-strand break repair and neurological disease. *DNA Repair (Amst)* 2008;7:1051–60.
44. Frappart PO, Lee Y, Lamont J, McKinnon PJ. BRCA2 is required for neurogenesis and suppression of medulloblastoma. *EMBO J* 2007;26:2732–42.
45. Frappart PO, et al. An essential function for NBS1 in the prevention of ataxia and cerebellar defects. *Nat Med* 2005;11:538–44.
46. Tronche F, et al. Disruption of the glucocorticoid receptor gene in the nervous system results in reduced anxiety. *Nat Genet* 1999;23:99–103.
47. Huse JT, Holland EC. Targeting brain cancer: advances in the molecular pathology of malignant glioma and medulloblastoma. *Nat Rev Cancer* 2010;10:319–31.
48. Monje M, Beachy PA, Fisher PG. Hedgehogs, flies, Wnts and MYCs: the time has come for many things in medulloblastoma. *J Clin Oncol* 2011;29:1395–8.
49. Northcott PA, et al. Medulloblastoma comprises four distinct molecular variants. *J Clin Oncol* 2011;29:1408–14.
50. Cho YJ, et al. Integrative genomic analysis of medulloblastoma identifies a molecular subgroup that drives poor clinical outcome. *J Clin Oncol* 2011;29:1424–30.